PALEOCEANOGRAPHY, VOL. 14, NO. 3, PAGES 360-373, JUNE 1999

19449186, 1999, 3, Downloaded from https://agupubs.onlinelibrary.wiley.com/doi/10.1029/1999PA900001 by Mbl Whoi Library, Wiley Online Library on [11/11/2022]. See the Terms and Conditions (https://onlinelibrary.wiley.com/terms-and-conditions) on Wiley Online Library for rules of use; OA articles are governed by the applicable Creative Commons License

A geostrophic transport estimate for the Florida Current from the oxygen isotope composition of benthic foraminifera

Jean Lynch-Stieglitz

Department of Earth and Environmental Sciences, Lamont-Doherty Earth Observatory of Columbia University
Palisades, New York

William B. Curry

Woods Hole Oceanographic Institution, Woods Hole, Massachusetts

Niall Slowey

Department of Oceanography, Texas A & M University, College Station, Texas

Abstract. We present a new method for the quantitative reconstruction of upper ocean flows for during times in the past. For the warm (T>5°C) surface ocean, density can be accurately reconstructed from calcite precipitated in equilibrium with seawater, as both of these properties increase with decreasing temperature and increasing salinity. Vertical density profiles can be reconstructed from the oxygen isotopic composition of benthic foraminifera. The net volume transport between two vertical density profiles can be calculated using the geostrophic method. Using benthic foraminifera from surface sediment samples from either side of the Florida Straits (Florida Keys and Little Bahama Bank), we reconstruct two vertical density profiles and calculate a volume transport of 32 Sv using this method. This agrees well with estimates from physical oceanographic methods of 30-32 Sv for the mean annual volume transport. We explore the sensitivity of this technique to various changes in the relationship between temperature and salinity as well as salinity and the oxygen isotopic composition of seawater.

1. Introduction

Ocean circulation plays a crucial role in the distribution of heat and carbon within the ocean/atmosphere system. Accurate reconstruction of ocean flow fields for times in the geologic past not only will provide us with a better understanding of these past climate regimes but will help to validate the ability of ocean and atmospheric models to simulate climate regimes different from the present. Qualitative information about deep water sources and paths during times in the past is inferred from tracer (carbon isotope and trace metals) distributions as recorded by benthic foraminifera [e.g., *Boyle and Keigwin*, 1987; *Duplessy et al.*, 1988; *Boyle*, 1992; *Lynch-Stieglitz and Fairbanks*, 1994; *Sarnthein et al.*, 1994]. Quantitative information about deep water flow (residence times) is obtained from paired radiocarbon analyses on benthic and planktonic foraminifera [e.g., *Broecker et al.* 1988; *Shackleton et al.*, 1988; *Adkins and Boyle*, 1997]. Sediment properties can yield some qualitative information about near-bottom oceanic currents but can be difficult to relate to the large-scale flow. For example, *Gardner et al.* [1989] find sedimentological evidence for southward flowing near-bottom currents in the Florida Straits, while the vast majority of waters travel northward through the Florida Straits. The positions of major surface water flows such as the North Atlantic Drift can be inferred on the basis of reconstructions of the oceanographic fronts along which they travel [e.g., *McIntyre et al.*, 1976]. However, there is no existing method for the quantitative reconstruction of upper ocean transports.

Here we propose a new method for estimating transport in the upper ocean for times in the past via the reconstruction of the density structure of the upper ocean. Vertical density profiles can be reconstructed using oxygen isotope measurements on benthic foraminifera from cores collected from a range of depths. The mean flow of large-scale low-frequency ocean currents can be reconstructed from density gradients within the ocean using the geostrophic method. The reliability of this method, in which a vertical profile of velocity is reconstructed from two adjacent density profiles, was demonstrated by *Wust* [1924] using hydrographic data in the Florida current along with direct current measurements obtained by *Pillsbury* [1891]. The geostrophic method has since become a standard tool in physical oceanography and has been successfully applied in numerous oceanographic regimes. While closely spaced density profiles are necessary for a detailed reconstruction of the flow velocity, the mean velocity or transport between the two profiles does not depend on the details of the density structure between the two profiles. In this way the vertical distribution of transport, as well as net transport relative to an assumed reference level, can be calculated through a section defined by only two vertical density profiles.

[1]Isotopic data are available electronically at the World Data Center-A for Paleoclimatology, NOAA/NGDC, 325 Broadway, Boulder, Colorado (ftp://ftp.ngdc.noaa.gov/paleo/contributions_by_author/lynch-stieglitz1999).

Copyright 1999 by the American Geophysical Union.

Paper number 1999PA900001.
0883-8305/99/1999PA900001$12.00

The oxygen isotopic composition of foraminifera has been used as an indicator of paleo-temperature by paleoceanographers for 50 years, and the geostrophic method has been used by physical oceanographers for almost 80 years. Here, for the first time, we bring these two tools together and present a method for the quantitative reconstruction of upper ocean currents for the paleo-ocean.

2. The Geostrophic Method

2.1. Geostrophic Currents

Currents can be described as geostrophic when the Coriolis term (a function of the latitude and the velocity of the water) acting on a parcel of moving water is balanced by a horizontal pressure gradient force. This equilibrium situation is achieved in much of the ocean whether the primary forcing that maintains this equilibrium flow against eventual destruction by frictional forces is the wind or the generation of density differences themselves. In this way the steady state circulation of the ocean is reflected in the density distribution. If we look at a section of temperature from Bermuda to the Chesapeake Bay (Figure 1), we can see that in regions of strong northward flow (the Gulf Stream) the isotherms (and thus surfaces of constant density) are strongly deflected upward toward the continental margin of North America. This reflects the strong horizontal density gradient needed to balance the large Coriolis force (proportional to velocity). If we had information about the vertical temperature structure only from near Bermuda and from near the continental margin, we would not know where exactly the high-velocity region was, nor would we know whether there was a narrow high-velocity jet or a diffuse northward flow. However, the fact that temperatures were much colder for upper waters on the continental margin than they are off Bermuda would tell us that there was substantial net northward flow between these two locations.

2.2 Reconstructing Velocity and Transport Using the Geostrophic Method

If a flow is geostrophic (that is, reflects only the balance between the Coriolis force and horizontal pressure gradients), two density profiles can be used to generate a depth profile of

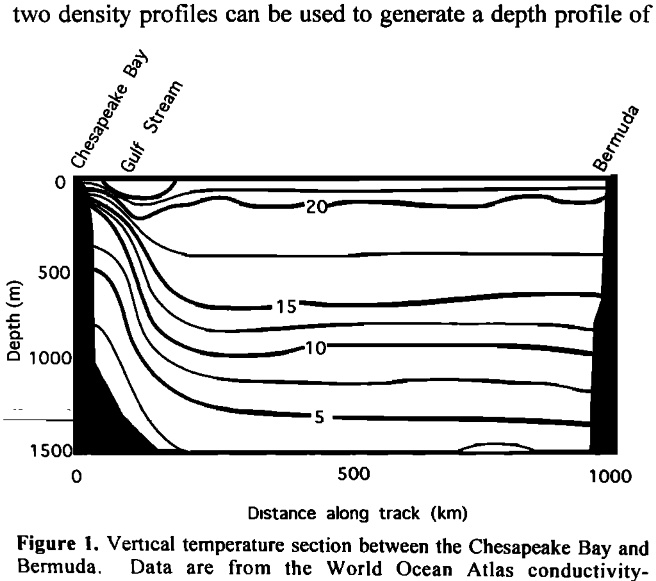

Figure 1. Vertical temperature section between the Chesapeake Bay and Bermuda. Data are from the World Ocean Atlas conductivity-temperature-depth (CTD) data set [*Levitus and Boyer*, 1994].

the average velocity between these two locations (the geostrophic method). Along with the two density profiles it is also necessary to know the velocity at one depth level as the geostrophic calculation will only produce relative velocity between two depths. Often a "level of no motion" is assumed at a certain depth with the depth chosen on the basis of the particular oceanographic location (often 1 or 2 km, the lower limit for wind-driven motions). No assumptions are made about the details of the density structure between the two profiles, and the actual average velocity is independent of the details of the flow/density structure between the two profiles. Oceanographers typically obtain a section, or line, of closely spaced vertical temperature and salinity profiles (from which density can be calculated) in order to reconstruct a detailed profile of velocity through this section. The section must be perpendicular to the axis of flow to reconstruct accurate velocities. This method has been applied to estimate flows of ocean currents, including the Gulf Stream, for 80 years. More recently, *Johns et al.* [1989] showed that the geostrophic transport of the Gulf Stream agrees with current profiler measurements to within 3%. In order to calculate the net volume transport across a section, two requirements for accurately reconstructing geostrophic velocity, the requirement that the section be perpendicular to the axis of flow and the requirement that the stations be closely enough spaced to sample the structure in the velocity field, can be relaxed. The net geostrophic transport between two widely spaced vertical profiles is often computed directly using a version of the geostrophic method which bypasses the calculation of velocity, the potential energy anomaly method [*Fofonoff*, 1962; *UNESCO*, 1991].

However, density estimates from benthic foraminifera will of necessity not result in a vertical profile, but rather will result in a slightly tilted one following the contours of the ocean bottom. Where the axis of flow is far from the continental margin (e.g., Figure 1) and the surfaces of constant density are horizontal in the vicinity of the core sites, this "pseudo-vertical" profile will be identical to a true vertical profile taken from above the deepest sample. Many core locations will, of necessity, be away from the main axis of the flow, in locations where the surfaces of constant density are nearly horizontal. If the flow is high at the core site, it is unlikely that an undisturbed stratigraphic sequence will exist. However, sometimes cores will be taken where the current extends to the continental margin, and thus the surfaces of constant density will not be horizontal. In these cases a geostrophic transport reconstruction using the pseudo-vertical density profile may introduce some error. However, tests using modern hydrographic data from a section through the Gulf Stream at the continental margin of Florida (29° N) where there is significant flow along the slope show that the geostrophic transport calculated using a pseudo-vertical margin profile reconstructed from the near-bottom hydrographic data differs from the transport calculated using the individual hydrographic stations by <1%.

3. Oxygen Isotope Ratios in Foraminifera as a Proxy for Density

The $\delta^{18}O$ in foraminifera has been thought of as a "paleo-thermometer" because the $\delta^{18}O$ of calcite ($\delta^{18}O_{calcite}$) in-

19449186, 1999, 3, Downloaded from https://agupubs.onlinelibrary.wiley.com/doi/10.1029/1999PA900001 by Mbl Whoi Library, Wiley Online Library on [11/11/2022]. See the Terms and Conditions (https://onlinelibrary.wiley.com/terms-and-conditions) on Wiley Online Library for rules of use; OA articles are governed by the applicable Creative Commons License

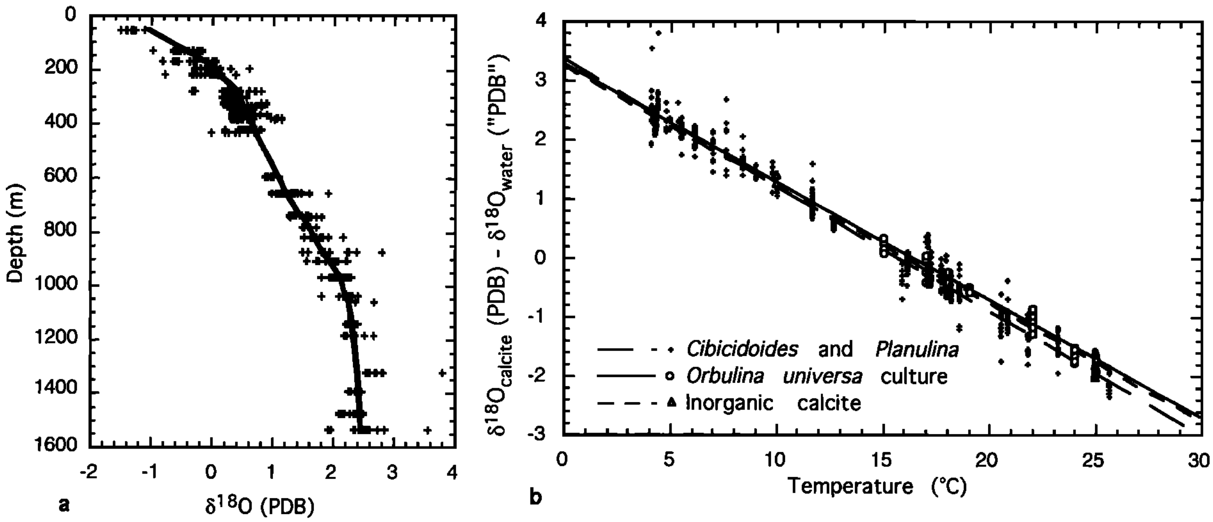

Figure 2. (a) The symbols are $\delta^{18}O$ of benthic foraminifera (genera *Planulina* and *Cibicidoides*) from surface sediments on the Little Bahama Bank [*Slowey and Curry*, 1995, *Curry et al.*, 1993]. The solid line is $\delta^{18}O_{calcite}$ of calcite precipitated in equilibrium with local seawater calculated from the experiments of *Kim and O'Neil* [1997]; $\delta^{18}O_{calcite} = \delta^{18}O_{water}(SMOW) - 0.27 + 3.25 - 0.20T$. Seawater $\delta^{18}O$ estimated from salinity using $\delta^{18}O_{water}$ (SMOW) $= -18.2 + 0.530S$, estimated using data from Geochemical Ocean Sections Study (GEOSECS) stations 29 and 37. (b) The isotopic fractionation, expressed as the difference between $\delta^{18}O_{calcite}$ and the $\delta^{18}O$ of seawater (converted from SMOW to a "Peedee Belemnite (PDB)" like scale by subtracting 0.27 in accordance with paleoceanographic tradition) versus temperature of calcification. Data from the Little Bahama Banks (small pluses) are shown along with the data from the foraminifera cultures of *Bemis et al.* [1998] (circles) and the inorganic precipitation experiments of *Kim and O'Neil* [1997] (triangles). While the true relationship between fractionation may not be linear over large temperature ranges, these data suggest that within the errors of the various data sets the relationship can approximated with a linear fit. The individual regressions for the three data sets are shown and are shown to be statistically indistinguishable (Table 1).

creases as calcification temperature decreases [*Emiliani*, 1955]. The $\delta^{18}O_{calcite}$ also reflects the $\delta^{18}O$ of the water ($\delta^{18}O_{water}$) in which the foraminifera grew. The fractionation between calcite precipitated inorganically and the water in which it forms increases by ~0.2‰ for every 1°C decrease in temperature [*O'Neil*, 1969; *Kim and O'Neil*, 1997]. In general, the isotopic composition of benthic foraminifera precipitated in seawater shows this relationship with temperature as well [*Shackleton*, 1974; *Herguera et al.*, 1992], but the absolute value of $\delta^{18}O_{calcite}$ may be shifted from the predicted inorganic value depending on the species analyzed. Using surface sediment samples and water column data from waters near the Bahamas spanning a temperature range of 4°-27°C, *Curry et al.* [1993] determined the oxygen isotope fractionation in the genera *Cibicidoides* and *Planulina* as a function of temperature (Figure 2). The water-calcite oxygen isotope fractionation data at 10° and 25°C from the inorganic precipitation studies of *Kim and O'Neil* [1997], obtained under conditions which are presumed to allow isotopic equilibrium, are indistinguishable from the fractionation data from the surface sediment *Cibicidoides* and *Planulina*. The regression (or "paleotemperature equation") obtained from the *Cibicidoides* and *Planulina* data is also statistically indistinguishable from that obtained from the fractionation versus temperature regression over the full range (10°-40°C) of the *Kim and O'Neil* [1997] experiments (Table 1). On the basis of core-top values from deeper waters, *Bemis et al.* [1998] also conclude that *Cibicidoides* appear to calcify near equilibrium, as determined by extrapolating the fractionation data of *Kim and O'Neil* [1997] to low temperatures.

Because the $\delta^{18}O_{calcite}$ in a benthic foraminifera reflects not only the temperature but also the $\delta^{18}O$ of the water in which it grew, the $\delta^{18}O_{calcite}$ in foraminifera is an inaccurate paleothermometer without independent knowledge of isotopic composition of the water. The $\delta^{18}O$ of seawater ($\delta^{18}O_{water}$) primarily reflects patterns of evaporation and freshwater in-

Table 1. Regression of Fractionation Versus Temperature

	Reference	Slope	Standard Error	Intercept	Standard Error
Cibicidoides and *Planulina* surface sediment	this study	3.38	0.0272	-0.21	0.002
Orbulina universa culture	*Bemis et al.* [1998]	3.28	0.138	-0.20	0.007
Inorganic calcite experiments	*Kim and O'Neil* [1997]	3.25	0.144	-0.20	0.005

Regression is determined for fractionation (defined as $\delta^{18}O_{calcite}$ (PDB) – $\delta^{18}O_{water}$ (SMOW) + 0.27, where PDB is Peedee belemnite) against temperature (°C)

19449186, 1999, 3, Downloaded from https://agupubs.onlinelibrary.wiley.com/doi/10.1029/1999PA900001 by Mbl Whoi Library, Wiley Online Library on [11/11/2022]. See the Terms and Conditions (https://onlinelibrary.wiley.com/terms-and-conditions) on Wiley Online Library for rules of use; OA articles are governed by the applicable Creative Commons License

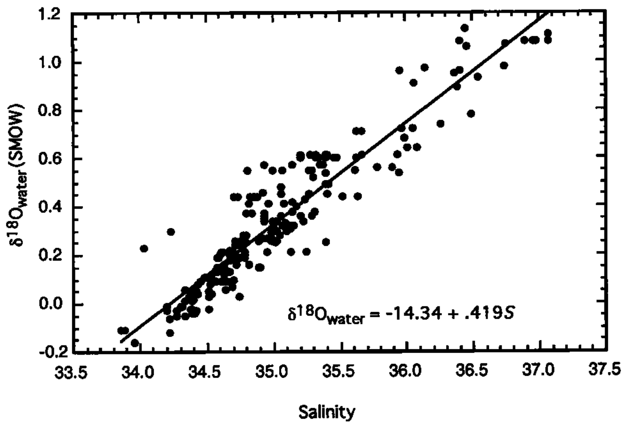

Figure 3. Oxygen isotopic composition and salinity of seawater from all GEOSECS open ocean stations for temperatures >5°C.

flux to the surface of the ocean. Because salinity also reflects these same processes, salinity and $\delta^{18}O_{water}$ are often well correlated in the ocean. Although the exact relationship varies in different areas of the surface ocean [e.g., *Craig and Gordon*, 1965; *Fairbanks et al.*, 1992], the vast majority of surface waters in the ocean have salinity and $\delta^{18}O_{water}$ which fall close to a linear trend [*Craig and Gordon*, 1965; *Broecker*, 1986]. Subsurface waters warmer than 5°C also fall along the surface water trend (Figure 3). The conservative properties of these upper and intermediate water masses reflect the surface water properties at the location of water mass formation, so it is not surprising that they fall along the same regression line as surface waters.

This linear relationship between $\delta^{18}O_{water}$ and salinity for the upper water masses of the World Ocean is a consequence of fundamental properties of the ocean-atmosphere system, specifically, the interplay between evaporation/precipitation patterns and the wind-driven ocean circulation. The linear relationship suggests the mixing of seawater with salinity and $\delta^{18}O_{water}$ characteristic of subthermocline waters with a fresh, low-$\delta^{18}O$ source. The net evaporation of water in the subtropics is primarily balanced by net precipitation in subpolar latitudes. *Craig and Gordon* [1965] suggest that the $\delta^{18}O$ of the freshwater end-member represents the mean isotopic composition of subpolar precipitation. Indeed, the isotopic composition of water in rivers flowing into the Arctic Ocean, which average precipitation from a large region, $\delta^{18}O$ = -21‰ [*Bauch et al.*, 1995], is very close to the Northern Hemisphere end-member postulated by *Craig and Gordon* [1965]. The river networks on land and the high-latitude ocean circulation serve to homogenize the salinity and $\delta^{18}O_{water}$ within the subpolar gyres. It is this homogenized end-member that mixes with the higher salinity water of the subtropical regions of the oceans, producing the linear relationship between $\delta^{18}O_{water}$ and salinity for each ocean region.

While we cannot separate the contributions of $\delta^{18}O_{water}$ (related to salinity, *S*) and temperature, *T*, on the $\delta^{18}O_{calcite}$, we can still calculate quite accurate density profiles from the $\delta^{18}O_{calcite}$. In fact, in today's ocean, density can be more accurately estimated from $\delta^{18}O_{calcite}$ than can temperature. This is because the compensating effects of temperature and salinity on $\delta^{18}O_{calcite}$ and density are very similar. Both $\delta^{18}O_{calcite}$ and density will increase as a result of increasing salinity or decreasing temperature. This is reflected in the fact that lines of constant $\delta^{18}O_{calcite}$ and lines of constant sigma-*T* are roughly parallel in *T-S* space (Figure 4). This relationship holds best at high temperatures where the effects of temperature on density are linear.

Figure 4 shows that with no knowledge of the temperature or salinity of a water mass, from the $\delta^{18}O_{calcite}$ of a foraminifera growing in this water we can estimate the density fairly accurately. If we have some knowledge of the local relationship between temperature and salinity, we can make an even better estimate of density. In a small geographic region where the *T-S* relationship is relatively tightly constrained, density can be predicted very accurately using $\delta^{18}O_{calcite}$.

The effects of temperature and salinity on seawater density as well as the effects of temperature on the isotopic fractionation during the precipitation of calcite are physical constants. However, for times in the geologic past our ability to reconstruct density from the $\delta^{18}O_{calcite}$ will be limited by our knowledge of the relationships between $\delta^{18}O_{water}$ and salinity as well as the relationships between temperature and salinity. For times in the relatively recent past, such as during the Holocene or even the Last Glacial Maximum, we can make fairly educated guesses as to how these relationships may change. However, for the more distant past where our knowledge of the ocean is poorer our density estimates will be less accurate.

4. The Florida Current

The Florida Current, which flows through the Florida Straits (Figure 5), is the southernmost part of the Gulf Stream. The average northward transport of the Florida Current is fairly well constrained by modern measurements at 30-32 Sv [*Hogg and Johns*, 1995, and references therein]. Although the Florida Current transport shows a seasonal variation with a 4.6 Sv range as well as considerable variability on short timescales [*Larsen*, 1992], *Schmitz and McCartney* [1993] as-

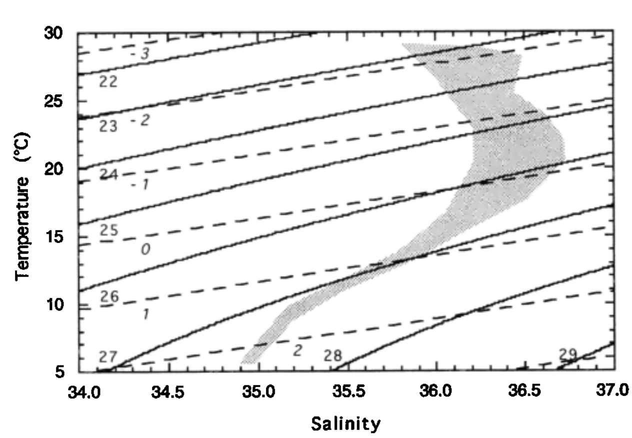

Figure 4. Lines of constant sigma-*T* (solid) and constant $\delta^{18}O$ of calcite tests of *Cibicidoides* and *Planulina* ($\delta^{18}O_{cib}$) (dashed) as a function of temperature and salinity in the upper ocean. *T-S* data from the Florida Straits fall within the stippled envelope [*Schmitz et al.*, 1993]. The $\delta^{18}O_{cib}$ was calculated as in Equation (1), assuming the relationship between $\delta^{18}O$ of seawater and salinity shown in Figure 3.

19449186, 1999, 3, Downloaded from https://agupubs.onlinelibrary.wiley.com/doi/10.1029/1999PA900001 by Mbl Whoi Library, Wiley Online Library on [11/11/2022]. See the Terms and Conditions (https://onlinelibrary.wiley.com/terms-and-conditions) on Wiley Online Library for rules of use; OA articles are governed by the applicable Creative Commons License

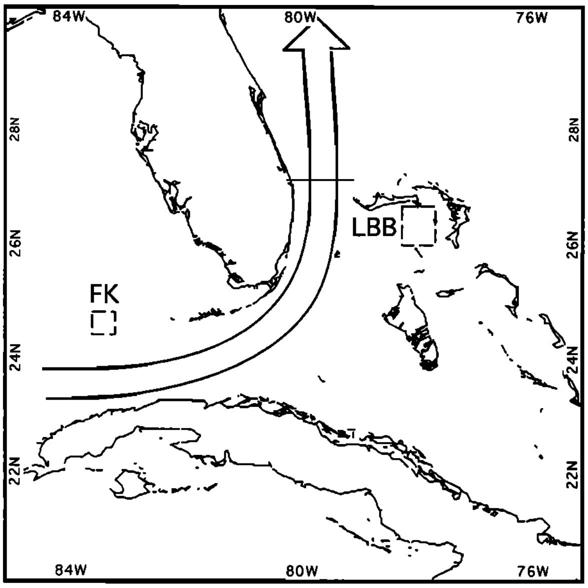

Figure 5. Location of surface sediment samples from the Little Bahama Banks (LBB) and Florida Keys (FK) located on either side of the Florida Current (arrow). Also indicated by a horizontal line is the location of the 27°N temperature and density sections shown in Figure 6.

sign an uncertainty of only 5% to the mean annual transport. The transport at the Florida Current includes 13 Sv of flow from the South Atlantic which will travel northward in the Gulf Stream and ultimately compensate the export of North Atlantic Deep Water (NADW) from the North Atlantic. The other 17 Sv compensate upper waters, which are recirculated from the eastern portion of the North Atlantic subtropical gyre [*Schmitz and McCartney*, 1993]. While the Gulf Stream flow increases to as much as 150 Sv farther north, this enhancement is due to smaller scale recirculations [*Hogg and Johns*, 1995]. The strong tilts in the surfaces of constant temperature and density within the Florida Straits reflect the geostrophic adjustment of the density surfaces in the presence of the large velocities (Figure 6). The contrasts in temperature and density across the Florida Current are large and should be well represented in the $\delta^{18}O_{calcite}$ of benthic foraminifera living in this region.

5. Methods

5.1. Oxygen Isotope Data

Here we estimate the geostrophic transport of the Florida Current using the density profiles reconstructed from oxygen isotope ratios in benthic foraminifera. As explained above, we need two vertical profiles on each side of the Florida Current. On the seaward side we will use measurements on benthic foraminifera from surface sediments near the Little Bahama Banks [*Slowey and Curry*, 1995; *Curry et al.*, 1993]. On the Florida side of the current we construct a profile from surface sediments near the Florida Keys (Figure 7). These surface sediment profiles should be representative of late Holocene conditions, so the transport estimate we derive can then be compared to modern estimates from physical oceanographic data. Because the flow in the Florida Straits is very nearly geostrophic and because the volume transport changes little downstream from a section across the straits near Florida Keys and across the straits at the Bahamas [*Richardson et al.*, 1969], we can use these two vertical profiles on either side of the Florida current to compute a geostrophic transport despite the fact that that the Bahamas profile is downstream from the Keys profiles. Profile locations are shown in Figure 5, and sample locations are listed in Table 2. Individual specimens of benthic foraminifera (genera *Planulina* and *Cibicidoides*) were isolated for isotopic analysis. All measurements were performed at Woods Hole Oceanographic Institution on a Finnigan MAT252 mass spectrometer equipped with an automated carbonate preparation device. The analytical procedures are detailed by Curry [1997].[1]

5.2 Estimating Density From $\delta^{18}O_{cib}$

5.2.1. Calculate sigma-*T* for *T-S* pairs in the Florida Straits. Most waters in the Florida Straits fall in a tightly constrained envelope in temperature-salinity space [*Schmitz et al.*, 1993] (Figure 4). From the *T-S* pairs in this water we first calculate sigma-*T* using the 1980 International Equation of State of Sea Water (IES 80) [*Millero and Poisson*, 1981].

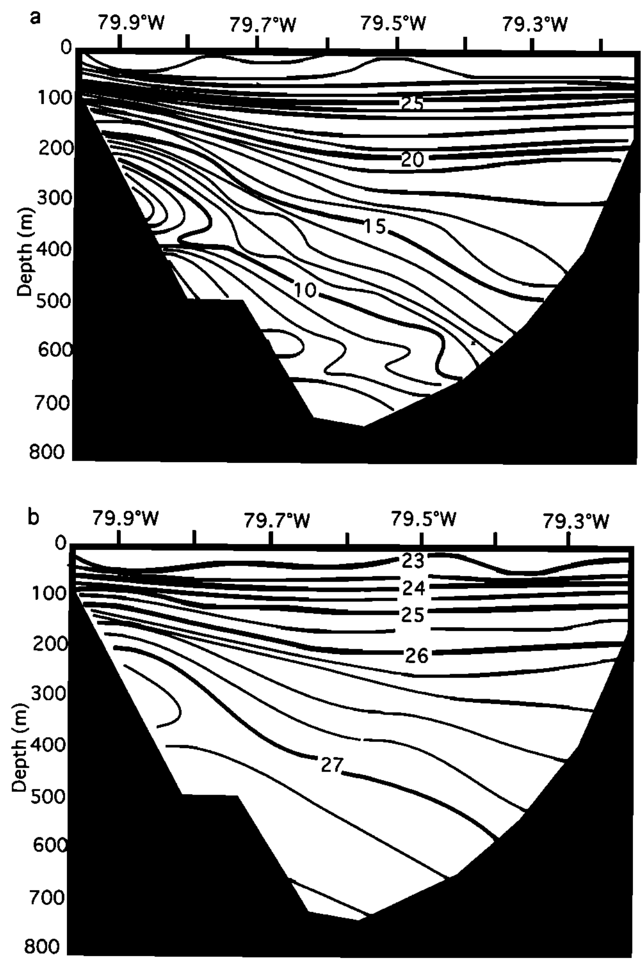

Figure 6. (a) Temperature and (b) sigma-*T* profiles at 27°N across the Florida current. Data are from the World Ocean Atlas CTD data set [*Levitus and Boyer*, 1994].

19449186, 1999, 3, Downloaded from https://agupubs.onlinelibrary.wiley.com/doi/10.1029/1999PA900001 by Mbl Whoi Library, Wiley Online Library on [11/1/2022]. See the Terms and Conditions (https://onlinelibrary.wiley.com/terms-and-conditions) on Wiley Online Library for rules of use; OA articles are governed by the applicable Creative Commons License

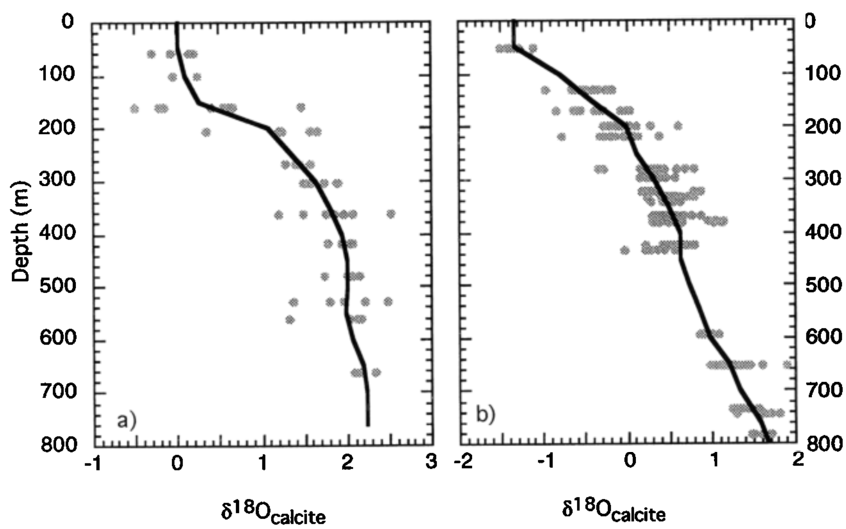

Figure 7. Measured $\delta^{18}O$ of surface sediment *Cibicidoides* and *Planulina* from (a) the Florida Keys and (b) the Little Bahama Banks. The symbols represent measurements of individual foraminifera, and the solid lines are the interpolated profiles used in the transport calculations.

5.2.2. Calculate $\delta^{18}O_{water}$ for each *T-S* pair. The oxygen isotopic composition of the water is predicted using the relationship between salinity and $\delta^{18}O_{water}$ for the waters warmer than 5°C from two nearby Geochemical Ocean Sections Study (GEOSECS) stations ($\delta^{18}O_{water}$ (SMOW) = -18.2 + 0.530*S*, Figure 8).

5.2.3. Calculate the predicted $\delta^{18}O$ of foraminifera calcifying in this water. The $\delta^{18}O$ expected for the foraminifera (*Planulina* and *Cibicidoides*), which also appears to be the $\delta^{18}O$ of calcite precipitated in equilibrium with seawater, is then calculated using the relationship derived from the *Planulina* and *Cibicidoides*) data shown in Figure 2 and Table 1:

$$\delta^{18}O_{cib} = [\delta^{18}O_{water}(SMOW) - 0.27] - 0.21T + 3.38 \qquad (1)$$

5.2.4. Determine relationship between $\delta^{18}O_{cib}$ and sigma-*T*. We derive an empirical relationship between the $\delta^{18}O_{cib}$ and sigma-*T* (Figure 8 and Table 3). Because this relationship depends on the local relationship between $\delta^{18}O_{water}$, salinity, and temperature, it will not necessarily hold outside today's North Atlantic subtropical gyre.

5.2.5. Compute density using $\delta^{18}O_{cib}$ measurements from surface sediment samples. We averaged the individual $\delta^{18}O_{cib}$ measurements for each surface sediment sample and then interpolated the average $\delta^{18}O_{cib}$ measurements to common depth levels (Table 4 and Figure 7). The uppermost $\delta^{18}O_{cib}$ averages were extrapolated to the sea surface. We convert to sigma-*T* using the above relationship for today's subtropical North Atlantic (Figure 8 and Table 3).

5.3. Calculating Geostrophic Transport

We calculate the geostrophic transport using the two density profiles and assuming a level of no motion at 760 m, the depth of the channel at the Florida Straits. Geostrophic transport can be calculated using the potential energy anomaly method as first formulated by *Fofonoff* [1962] and described by *UNESCO* [1991] and *Sato and Rossby* [1995]. The vertical distribution of the transport can be calculated using the modification of the potential energy anomaly method presented by *Sato and Rossby* [1995, equations (9) and (10)]. Because we have no independent knowledge of the depth distribution of temperature and salinity, instead of using the specific volume anomaly δ in these calculations we use the thermosteric anomaly $\Delta_{s,t}$, which can be calculated with a knowledge of sigma-*T* alone and is the dominant contribution to the specific volume anomaly in waters in the upper 1000 m of the ocean [*Pond and Pickard*, 1983]. This approximation makes only a small difference in the result.

6. Transport Estimates for the Florida Straits

6.1. Best Estimate

Using the methods described above, we calculate a transport through the Florida Straits of 32 Sv (Table 4), in good agreement with the long-term average transport estimates based on physical oceanographic methods (30-32 Sv). In addition, the vertical distribution of flow agrees well with modern measurements (Figure 9). The time period represented by our measurement is not well defined. Downcore records of $\delta^{18}O_{cib}$ from the Little Bahama Banks [*Slowey and Curry*, 1995] are quite constant for the Holocene, indicating that the density profile estimated for the Little Bahama Banks most likely is representative of the entire Holocene. We have no downcore records from the Florida Keys, but it is likely that the Holocene section is quite thick [e.g., *Locker and Hine*, 1995]. If this is the case, the data from Florida Keys profile may reflect as little as several hundred years. Downcore records and/or radiocarbon analyses could be used to constrain the timescale of the measurement.

The accuracy of our transport estimate is a direct consequence of the fact that we know the relationship between temperature, salinity, and $\delta^{18}O_{water}$ in this area and can use this information to accurately transform the $\delta^{18}O_{cib}$ data into density. This method could conceivably be used to reconstruct modern flows in areas where long term monitoring of flow is

19449186, 1999, 3, Downloaded from https://agupubs.onlinelibrary.wiley.com/doi/10.1029/1999PA900001 by Mbl Whoi Library, Wiley Online Library on [11/11/2022]. See the Terms and Conditions (https://onlinelibrary.wiley.com/terms-and-conditions) on Wiley Online Library for rules of use; OA articles are governed by the applicable Creative Commons License

Table 2. Sample Locations

Core	Depth, m	Latitude, °N	Longitude, °W	Sample Type
		Little Bahama Banks		
W120A-26G	53	26.59	77.93	grab sample
W120A-24G	129	26.42	77.93	grab sample
W120A-23G	169	26.59	77.93	grab sample
W120A-21G	199	26.59	77.94	grab sample
W120A-20G	218	26.59	77.94	grab sample
W120A-19G	281	26.58	77.95	grab sample
W120A-18G	281	26.57	77.97	grab sample
W120A-17G	298	26.58	77.96	grab sample
W120A-16G	322	26.57	77.97	grab sample
W120A-15G	334	26.57	77.97	grab sample
W120A-14G	343	26.57	77.97	grab sample
W120A-12G	368	26.57	77.97	grab sample
W120A-11G	379	26.56	77.97	grab sample
W120A-10G	383	26.56	77.97	grab sample
OC205-2-149	423	26.26	77.67	piston core
OC205-2-148	434	26.26	77.67	gravity core
OC205-2-48	595	26.24	77.68	box core
OC205-2-106	654	25.98	78.18	gravity core
OC205-2-69	735	26.23	77.69	box core
OC205-2-108	743	25.98	78.18	gravity core
OC205-2-33	783	26.22	77.69	gravity core
OC205-2-50	817	26.23	77.70	box core
OC205-2-70	876	26.22	77.70	box core
OC205-2-72	908	26.23	77.71	box core
OC205-2-103	965	26.07	78.06	gravity core
OC205-2-55	1140	26.17	77.71	box core
OC205-2-97	1183	25.94	77.85	gravity core
OC205-2-7	1320	26.14	77.74	gravity core
OC205-2-67	1392	26.15	77.74	box core
OC205-2-59	1477	26.17	77.74	box core
OC205-2-117	1535	26.03	77.88	gravity core
		Florida Keys		
C125A-6G	60	24.54	83.32	grab sample
C125A-7G	100	24.49	83.29	grab sample
C125A-8G	161	24.46	83.30	grab sample
C125A-9G	206	24.44	83.29	grab sample
C125A-10G	267	24.42	83.30	grab sample
C125A-11G	304	24.40	83.31	grab sample
C125A-12G	364	24.38	83.31	grab sample
C125A-13G	418	24.37	83.32	grab sample
C125A-14G	480	24.36	83.32	grab sample
C125A-15G	530	24.35	83.31	grab sample
C125A-16G	560	24.33	83.30	grab sample
C125A-17G	662	24.45	83.47	grab sample

not feasible but where a one-time collection of surface sediments, water column temperature, salinity, and $\delta^{18}O_{water}$ is possible. However, the most promise for this method lies in the reconstruction of upper ocean flows during times in the past for which few satisfactory methods of reconstructing upper ocean flow exist. What follows are the results of sensitivity studies designed to evaluate how well we can estimate past flows using this method given the uncertainties in our knowledge of the relationship between temperature, salinity, and $\delta^{18}O_{water}$.

6.2. Sensitivity Calculations

While we can assume that the whole ocean salinity and $\delta^{18}O_{water}$ will increase as sea level drops, we have few accurate methods to reconstruct the past relationships between temperature, salinity, and $\delta^{18}O_{water}$ within the ocean that would have resulted from the changed oceanic and atmospheric circulation. How well do we have to know the temperature, salinity and $\delta^{18}O_{water}$ relationships in order to estimate density well enough for a meaningful transport estimate?

6.2.1. Using open ocean $\delta^{18}O_{calcite}$ versus sigma-T. While we used the T-S-$\delta^{18}O_{water}$ data from the western subtropical Atlantic Ocean in order to derive our best estimate for the transport through the Florida Straits, we argued earlier that because the compensating effects of salinity and temperature on $\delta^{18}O_{calcite}$ are similar to the compensating effects on density, we should be able to get a good estimate of density from $\delta^{18}O_{calcite}$ without knowing specifically how temperature and salinity contribute to the $\delta^{18}O_{calcite}$ measured in the foraminifera. When we use $\delta^{18}O_{water}$ from all open ocean waters warmer than 5°C measured by the GEOSECS program, along with the temperature and salinity measurements collected at the same time, we can derive a general relationship between $\delta^{18}O_{cib}$ and sigma-T for the entire upper open ocean (Figure 10). The global relationship is quite well constrained despite the varying T-S-$\delta^{18}O_{water}$ relationships for the individual ocean regions. Again, this reflects the fact that whether because of higher salinity or colder temperatures, a higher $\delta^{18}O_{cib}$ reflects more dense waters. Using this relationship results in a transport estimate of 33 Sv (Table 3).

6.2.2. Using regional $\delta^{18}O_{cib}$ versus sigma-T. To try to get a more representative understanding of how regional differences in the relationship between temperature, salinity and $\delta^{18}O_{water}$ will influence transport estimates, we will look to the data from the individual regions in today's ocean. While the details of the T-S-$\delta^{18}O_{water}$ relationship may change from ocean basin to ocean basin, there are similarities for warm waters in all basins and hemispheres (Figures 11a and 11b). Evaporation in the subtropical gyres produces relatively high salinity and $\delta^{18}O_{water}$, whereas waters originating in subpolar regions reflect enhanced precipitation and colder temperatures (lower salinity and $\delta^{18}O_{water}$). Despite the regional dissimilarities in the exact values of these properties, the relationship between $\delta^{18}O_{cib}$ and sigma-T is similar for all four regions shown (Figure 11c). Using these relationships from the "wrong" oceanic region to predict density from $\delta^{18}O_{cib}$ data from the Florida Straits and then estimating the transport through the Florida Straits results in transport estimates between 28 and 44 Sv (Table 3).

6.2.3. Assuming changed open ocean $\delta^{18}O_{water}$ versus salinity. While the dependence of $\delta^{18}O_{cib}$ on temperature and of sigma-T on temperature and salinity are based on relatively simple physical principles that will not change with time, the dependence of $\delta^{18}O_{cib}$ on salinity depends on the relationship between $\delta^{18}O_{water}$ and salinity. This relationship results from the complex interplay between evaporation, precipitation and mixing processes within the ocean and atmosphere [*Craig and Gordon*, 1965]. While we have examined the impact of the different $\delta^{18}O_{water}$-S relationships in various regions of today's ocean (spatial variability), it is also possible that this relationship could have changed with time. The simplest possible way to interpret the upper water $\delta^{18}O_{water}$ and salinity data is as a mixing line that is constrained to intersect both the $\delta^{18}O_{water}$ and salinity of upwelled subthermocline water and some sort of "average" $\delta^{18}O$ value for precipitation over the

19449186, 1999, 3, Downloaded from https://agupubs.onlinelibrary.wiley.com/doi/10.1029/1999PA900001 by Mbl Whoi Library, Wiley Online Library on [11/11/2022]. See the Terms and Conditions (https://onlinelibrary.wiley.com/terms-and-conditions) on Wiley Online Library for rules of use; OA articles are governed by the applicable Creative Commons License

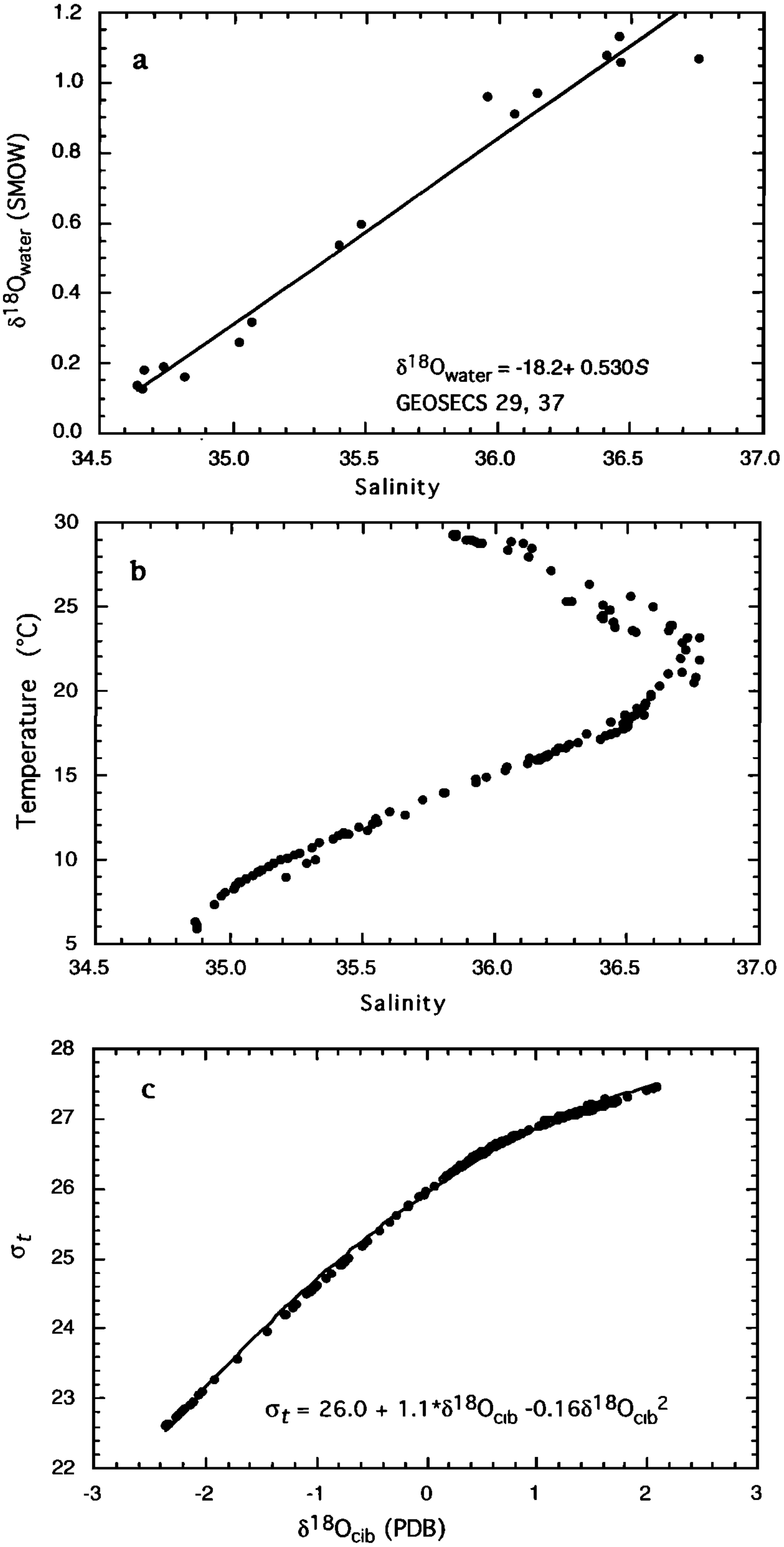

Figure 8. (a) Salinity and $\delta^{18}O_{water}$ data from GEOSECS stations 29 and 37 (western subtropical North Atlantic) for the waters warmer than 5°C and linear regression through this data, (b) *T-S* data from the Florida Straits, and (c) calculated $\delta^{18}O$ of *Planulina* and *Cibicidoides* precipitated in these waters (using regression in Figure 8a and equation (1)) versus sigma-*T* (1980 International Equation of State of Sea Water) [*Millero and Poisson*, 1981] for each *T*, *S* pair shown in Figure 8b. Also shown is the second-order polynomial fit we use to transform $\delta^{18}O_{cib}$ to sigma-*T* estimates. This relationship, based on seawater data in the same region, is used in the best transport estimate for the Florida Current (Figure 9).

19449186, 1999, 3, Downloaded from https://agupubs.onlinelibrary.wiley.com/doi/10.1029/1999PA900001 by Mbl Whoi Library, Wiley Online Library on [11/11/2022]. See the Terms and Conditions (https://onlinelibrary.wiley.com/terms-and-conditions) on Wiley Online Library for rules of use; OA articles are governed by the applicable Creative Commons License

Table 3. Transport Estimate Summary

	Data Sources	$\delta^{18}O_{water} = a + bS$		$\sigma_t = a + b\delta^{18}O_{cib} + c\delta^{18}O_{cib}^2$			Total Transport, Sv
		a	*b*	*a*	*b*	*c*	
Physical Oceanographic Estimates	---	---	---	---	---	---	30-32
Best estimate	Relationship between salinity and $\delta^{18}O_{water}$ from subtropical western Atlantic GEOSECS (29 and 37). *T-S* pairs from Florida Straits CTD profiles	-18.2	0.530	26.0	1.1	0.16	32
Global Open Ocean	measured $\delta^{18}O_{water}$ for all open ocean waters, T>5°C (GEOSECS), and *T-S* from these locations	-14.3	0.419	25.8	1.1	0.15	33
Using wrong regional properties:							
North Pacific	measured $\delta^{18}O_{water}$ for GEOSECS 343, 345, and 347; T>5°C; and *T-S* from these locations	-11.1	0.322	25.4	1.0	0.03	44
South Pacific	measured $\delta^{18}O_{water}$ for GEOSECS 303 and 306, T>5°C; and *T-S* from these locations	-18.3	0.534	25.7	1.1	0.19	28
South Indian	measured $\delta^{18}O_{water}$ for GEOSECS 438; T>5°C; and *T-S* from these locations	-20.8	0.603	25.8	1.1	0.14	33
Modifications of Global Open Ocean							
4 ‰ lower fresh end member	*T-S* for all open ocean waters, T>5°C (GEOSECS)	-18.0	0.524	25.7	1.0	0.12	35
4 ‰ higher fresh end member	*T-S* for all open ocean waters; T>5°C (GEOSECS)	-10.0	0.294	25.9	1.0	0.15	28
No knowledge of $\delta^{18}O_{water}$ -*T-S*	Mean ocean values ($\delta^{18}O_{water}$ = 0.0 and S = 34.7)	---	---	25.5	1.1	0.10	39

GEOSECS, Geochemical Ocean Sections Study; CTD, conductivity-temperature-depth.

19449186, 1999, 3, Downloaded from https://agupubs.onlinelibrary.wiley.com/doi/10.1029/1999PA900001 by Mbl Whoi Library, Wiley Online Library on [11/11/2022]. See the Terms and Conditions (https://onlinelibrary.wiley.com/terms-and-conditions) on Wiley Online Library for rules of use; OA articles are governed by the applicable Creative Commons License

Table 4. Transport Calculation

Depth	Florida Keys Foraminifera $\delta^{18}O$	Sigma-T	Little Bahama Banks Foraminifera $\delta^{18}O$	Sigma-T	Transport, Sv	Transport/Unit Depth, Sv m^{-1}
0	0.03	25.98	-1.34	24.22	2.6	0.104
50	0.03	25.98	-1.34	24.22	4.5	0 090
100	0.10	26.06	-0.80	24.98	4.0	0.080
150	0 26	26.22	-0 44	25 45	3.6	0.073
200	1.08	26.93	-0.02	25.93	3 3	0.066
250	1.36	27.12	0.11	26.07	2 9	0.058
300	1 63	27.28	0.32	26.28	2.5	0.050
350	1.79	27.37	0.48	26.43	2.1	0.043
400	1.94	27.43	0.62	26.56	1.8	0.036
450	2.00	27.46	0.63	26 57	1 4	0.029
500	2.01	27.47	0.74	26.66	1.1	0.022
550	1 99	27.46	0.85	26.75	0.8	0.017
600	2 08	27.49	0.98	26.85	0.6	0.012
650	2.20	27.54	1.22	27.03	0.4	0.007
700	2.23	27.55	1.34	27.11	0.2	0 003
760	2.23	27.55	1.60	27 26	0.0	0.000

Total Transport is 31.9

subpolar latitudes (S=0), or the "fresh end-member" [*Craig and Gordon*, 1965]. During times in the past, such as the Last Glacial Maximum, the $\delta^{18}O_{water}$ and salinity of subthermocline water would have increased slightly because of the buildup of the continental ice sheets. The $\delta^{18}O$ of the fresh end-member could have changed because of changes in the temperature contrast between low and high latitudes among other factors. Snow trapped on the permanent ice caps in Antarctica and Greenland indicated that the $\delta^{18}O$ of precipitation at very high latitudes was between 5 and 10‰ lower during the last ice age. General circulation model studies [e.g., *Joussame and Jouzel*, 1993] suggest that this extreme depletion over the ice caps may have been accompanied by a more general but less extreme depletion in the subpolar latitudes. To represent the uncertainty in the $\delta^{18}O_{water}$ relationship due to this sort of variability in the fresh end-member, we estimate how the warm surface ocean $\delta^{18}O_{water}$ relationship would have changed because of a fresh end-member that is 4‰ lighter and 4‰ heavier than today's. We then recalculate the global warm ocean relationship between $\delta^{18}O_{cib}$ and sigma-T (Figure 12). The resulting range in the Florida Straits transport estimates is 28-35 Sv (Table 3).

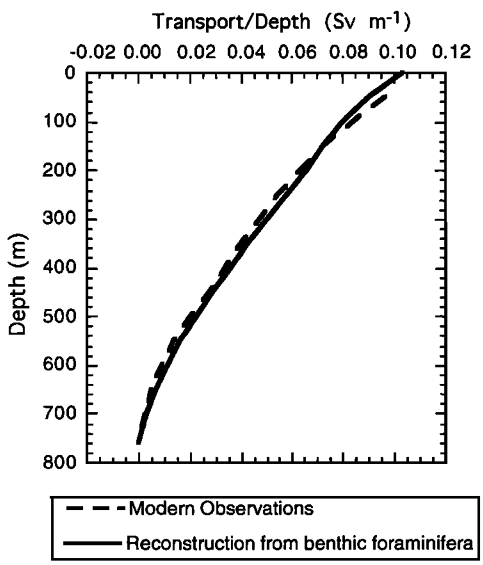

Figure 9. Best estimate Florida Straits volume transport per unit depth (solid line) with a total volume transport of 32 Sv. Also shown is volume transport per unit depth from current profilers (dashed line) [*Leaman et al*, 1989].

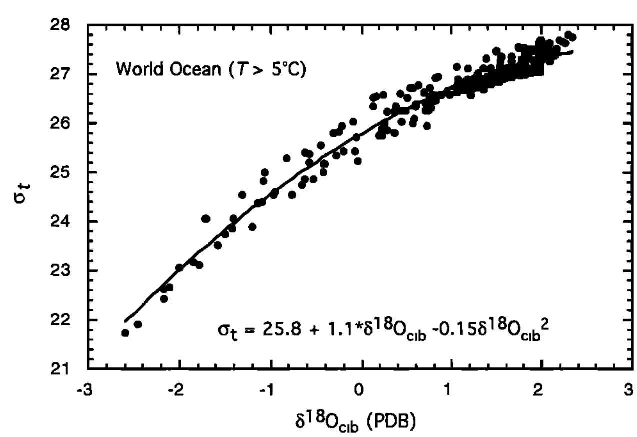

Figure 10. Sigma-T versus $\delta^{18}O_{cib}$ relationship for the warm ocean (T>5°C). Temperature, salinity, and $\delta^{18}O_{water}$ data are from open ocean GEOSECS stations in all three ocean basins where T>5°C. The isotopic composition of *Planulina* and *Cibicidoides* precipitated in these upper waters is calculated using (1) and the GEOSECS $\delta^{18}O_{water}$ and temperature data. Sigma-T is calculated using the temperature and salinity data from the sample locations. The $\delta^{18}O_{water}$ versus salinity relationship for these samples is shown in Figure 3.

19449186, 1999, 3, Downloaded from https://agupubs.onlinelibrary.wiley.com/doi/10.1029/1999PA900001 by Mbl Whoi Library, Wiley Online Library on [11/11/2022]. See the Terms and Conditions (https://onlinelibrary.wiley.com/terms-and-conditions) on Wiley Online Library for rules of use; OA articles are governed by the applicable Creative Commons License

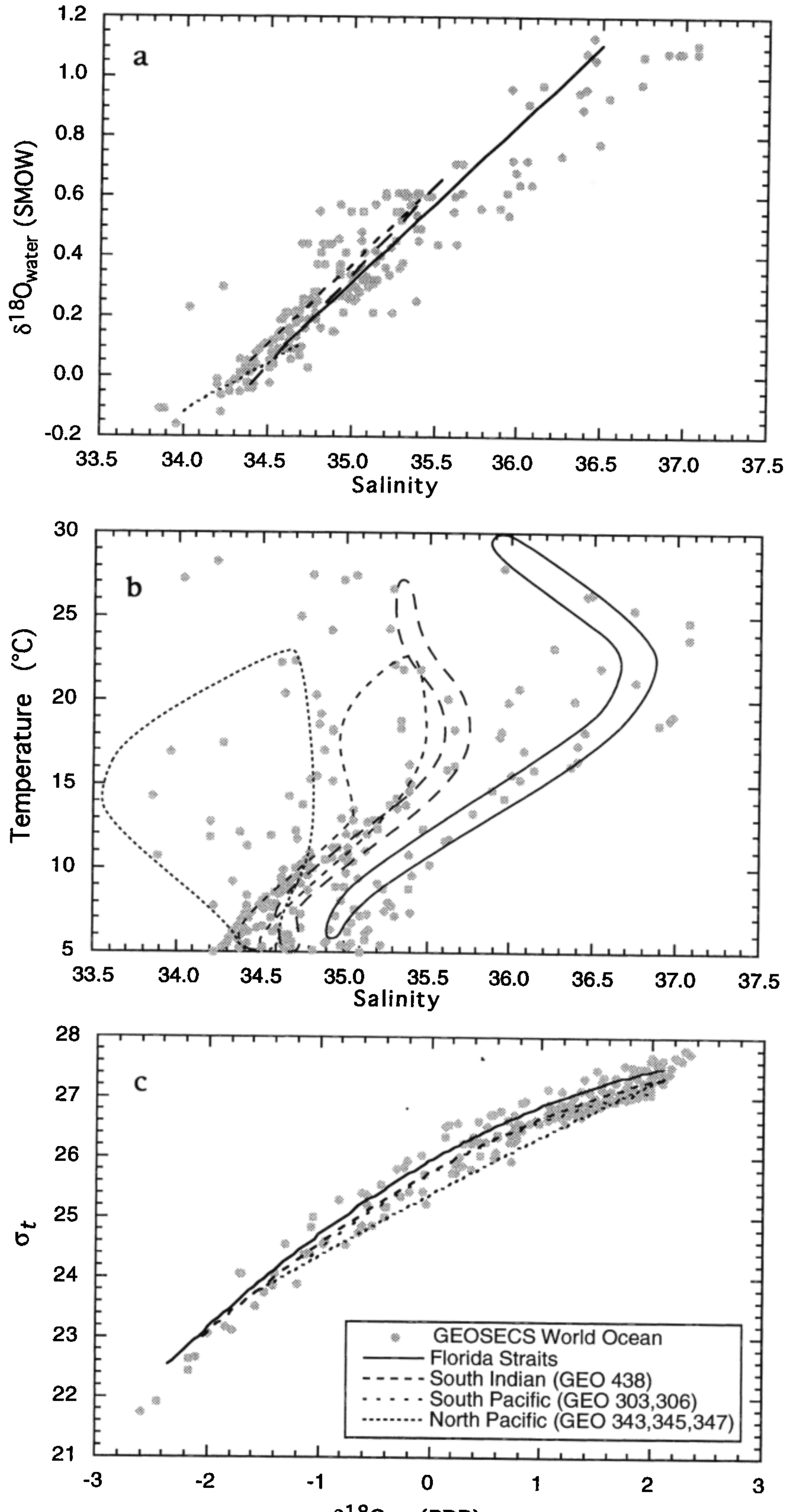

Figure 11. Relationship between sigma-T and $\delta^{18}O_{cib}$ for upper (T>5°C) waters in individual regions of the World Ocean. Trends for individual oceanic regions are shown in the solid lines. The shaded circles are data from the entire upper ocean (Figure 10), redrawn here for reference. T and S data and the $\delta^{18}O_{water}$ versus S relationship for the Florida Straits is the same as in Figure 8. For the Indian and Pacific Oceans, data from the individual GEOSECS stations listed in Table 3 are used.

19449186, 1999, 3, Downloaded from https://agupubs.onlinelibrary.wiley.com/doi/10.1029/1999PA900001 by Mbl Whoi Library, Wiley Online Library on [11/11/2022]. See the Terms and Conditions (https://onlinelibrary.wiley.com/terms-and-conditions) on Wiley Online Library for rules of use; OA articles are governed by the applicable Creative Commons License

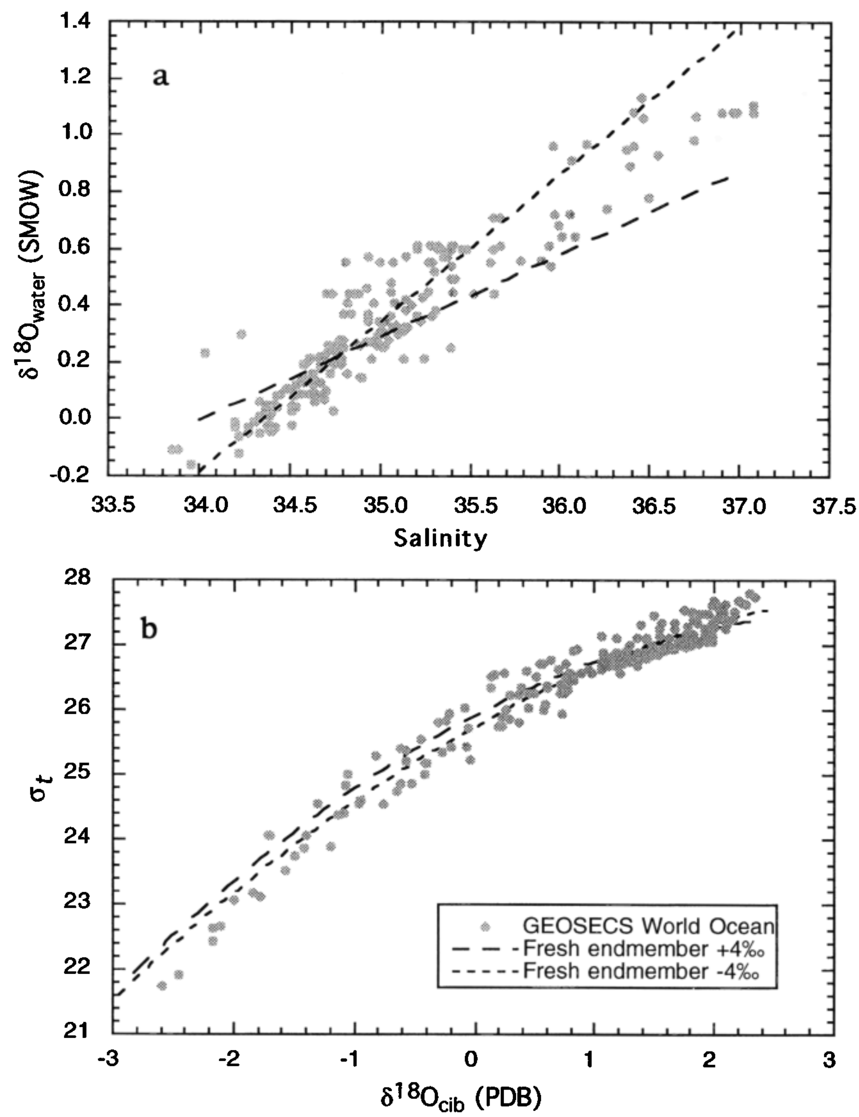

Figure 12. Relationship between sigma-T and $\delta^{18}O_{cib}$ for a hypothetical ocean where the $\delta^{18}O$ of precipitation falling in the subpolar regions is 4‰ higher and lower than today. This is the magnitude of change expected in the $\delta^{18}O$ of high latitude precipitation between today and, for example, the Last Glacial Maximum. The shaded circles are data from the entire upper ocean (Figure 10), redrawn here for reference.

6.2.4. Assume no knowledge of the surface ocean relationship between temperature, salinity and $\delta^{18}O_{water}$. From the above sensitivity studies it appears that when using the full range of different relationships between temperature, salinity and $\delta^{18}O_{water}$ observed in the open ocean and varying the oceanic $\delta^{18}O_{water}$-S relationship within reasonable limits, the resulting $\delta^{18}O_{cib}$ versus density relationships yield transport estimates ranging from 4 Sv lower to 12 Sv higher than the actual transport. Can one get a reasonable transport estimate without knowing anything about the T-S-$\delta^{18}O_{water}$ relationship within the ocean? How well can the transport be estimated by simply ascribing all of the structure in $\delta^{18}O_{cib}$ to temperature changes? We do this by recalculating the $\delta^{18}O_{cib}$ versus sigma-T relationship over a temperature range of 5°-30°C for seawater of mean ocean salinity (34.6) and $\delta^{18}O_{water}$ (0‰). The resulting transport estimate is 39 Sv. This works moderately well for today's ocean because for most of the surface ocean the modern S-$\delta^{18}O_{water}$ relationship is such that the estimated density is similar whether $\delta^{18}O_{calcite}$ contrasts are ascribed to temperature or salinity (Figure 4).

One of the reasons that the transport estimate is relatively immune to the changes in the relationship between $\delta^{18}O_{cib}$ and sigma-T is that, particularly, in a small region where the T-S relationship is relatively tight, while we may not know exactly to what density a particular $\delta^{18}O_{cib}$ corresponds, we will make the same error for both profiles. Because the geostrophic calculation depends only on the differences in density, the errors for each profile will tend to cancel each other out.

7. Utility of Method in Past Oceans

For the relatively recent past, such as the Last Glacial Maximum, there is no evidence for radical changes in atmos-

19449186, 1999, 3, Downloaded from https://agupubs.onlinelibrary.wiley.com/doi/10.1029/1999PA900001 by Mbl Whoi Library, Wiley Online Library on [11/11/2022]. See the Terms and Conditions (https://onlinelibrary.wiley.com/terms-and-conditions) on Wiley Online Library for rules of use; OA articles are governed by the applicable Creative Commons License

pheric and thus surface ocean circulation. Although the patterns of atmospheric and surface ocean circulation might have shifted in latitude, we still expect that there existed an evaporative subtropical gyre and a fresh subpolar gyre during even the periods of maximum glaciation. While the changes in oceanic and atmospheric circulation could have resulted in a glacial *T-S* relationship in the subtropical Atlantic Ocean different from today's, once we account for the whole ocean changes in salinity due to the ice sheet buildup, we imagine that the difference between glacial and modern property distributions at any one location was probably no larger than the differences between the different ocean basins today. Using this assumption, we estimate that the uncertainty in a transport estimate due to the incomplete knowledge of the *T-S*-$\delta^{18}O_{water}$ distributions within the glacial ocean will be comparable to the error in transport when we calculated it using the $\delta^{18}O_{cib}$ versus sigma-*T* relationships for different ocean basins (Table 3). While uncertainties in the $\delta^{18}O_{water}$-*S* relationship due to changes in the $\delta^{18}O$ of the fresh end-member can also be important, the expected temporal (e.g. glacial-interglacial) changes in the $\delta^{18}O$ of the fresh end-member are no larger than the range for different oceanographic regions today. In essence, we have come to the same conclusion as *Craig and Gordon* [1965] who, without the benefit of general circulation models or isotopic measurements on glacial ice, write that [*Craig and Gordon*, 1965, p. 65]

> Our discussion leads us to conclude that the isotopic variations in surface ocean waters may well be about the same in both glacial and non-glacial periods. (Of course the absolute oceanic values for δ and S shift along a slope somewhat similar to the high latitude surface water δ-S slope with the addition and removal of water from the oceans by the continental glaciers. Also there are transients during the growth and decay periods because of the mixing time between surface and deep waters. We speak here of the variations in the surface ocean waters at any given time). . . . We do not wish to discuss the effects of glaciation on ocean mixing and precipitation and evaporation, as these effects are very complicated. But for applications to paleotemperatures, it is probably most reasonable to assume that variations fairly similar to those seen today have generally been present in the surface ocean waters.

Independent knowledge of temperature from the benthic foraminifera, perhaps from Mg/Ca ratios [*Rosenthal et al.*, 1997], or *T*-$\delta^{18}O_{water}$ relationships estimated for surface waters in the region of upper water ventilation [*Labeyrie et al.*, 1992] can help to constrain the *T-S* relationship and to reduce this source of uncertainty.

While this method shows great promise for the reconstruction of oceanic volume transport during times in the past, it is also important to note its limitations. Transport estimates will be limited to upper waters and to relatively warm waters. While deepwater flows can also be largely geostrophic, the density contrasts in the deep ocean are much smaller and cannot be discerned given the amount of "noise" in the ability of foraminifera to record the temperature and $\delta^{18}O_{water}$ of its surroundings (Figure 2) . While this method can be used for flow in cold regions, in these regions the sigma-*T* becomes relatively insensitive to temperature, whereas the $\delta^{18}O_{calcite}$ will still become heavier with decreasing temperature (Figure 4). Because of this, an increase in $\delta^{18}O_{calcite}$ does not translate into a significant increase in density. In this situation it would be necessary to have a separate measure of temperature (e.g., Mg/Ca in the benthic foraminifera). In high latitudes another potential complication is the decoupling of $\delta^{18}O_{water}$ from salinity. While sea ice formation and melt will change salinity, the $\delta^{18}O_{water}$ is left relatively unaffected, further degrading the density estimate from $\delta^{18}O_{calcite}$. The best hope for accurate flow reconstructions using this method is in the oceanic warm sphere, those waters 5°C and above.

Another limitation of this method is geographical: in order to reconstruct flow one needs a vertical density profile on either side of the main flow. Many currents travel along an ocean boundary, and one density profile can be from the continental margin. However, the other profile will probably need to be from an island or shallow seamount. It is important to note that while we have shown a relatively constricted flow in this example, the two density profiles can be quite widely spaced in longitude even if there are flow reversals between the two density profiles. The calculated transport will be the net transport between these two profiles. One way around the problem of needing an island or continental boundary to construct a density profile is to use planktonic foraminifera. Planktonic foraminifera live at different depths in the water column and generally have $\delta^{18}O_{calcite}$ in equilibrium with the seawater in which they grow [*Emiliani*, 1954; *Fairbanks et al.*, 1982]. Some efforts have been made to use $\delta^{18}O_{calcite}$ from planktonic foraminifera for qualitative estimates of geostrophic flow [*Ortiz et al.*, 1997]. However, before planktonic foraminifera can be used for quantitative flow reconstruction a method for determining the depth at which they calcify is needed.

8. Conclusions

In this study we have shown that (1) the oxygen isotopic composition of calcite precipitated in equilibrium with modern seawater is an excellent proxy for the density of seawater. (2) Over a temperature range of 5°-27 °C, benthic foraminifera of the genera *Cibicidoides* and *Planulina* calcify close to isotopic equilibrium with seawater. (3) Transport estimates for the Florida Straits using density profiles reconstructed from benthic foraminifera and the geostrophic method agree very well with estimates from more conventional physical oceanographic techniques. (4) The use of this method is most accurate in the warm (*T*>5°C) surface ocean. Finally, (5) this method can be used for estimates of transport during the past, but uncertainties will be introduced because of changes in the distribution of the temperature, salinity, and $\delta^{18}O$ of seawater.

Acknowledgments. This work would not have been conceived without the time and freedom allowed by a WHOI postdoctoral fellowship to JL-S. This work was also supported by U.S. National Science Foundation grants OCE-9402804 and OCE-9503135 to WBC and OCE-9712147 to JL-S. We also thank P Lohmann and the Sea Education Association for collecting the grab samples from the *Westward* 120 and the *Cramer* 125 cruises and D. Ostermann for help with the sample preparation and analyses. We are also grateful to T. Rossby for his suggestions on the transport calculations and a thorough review of the manuscript, and to C. Schaefer-Neth and M. Delaney for their helpful comments on the manuscript. This is LDEO contribution 5899 and WHOI contribution 9876

19449186, 1999, 3, Downloaded from https://agupubs.onlinelibrary.wiley.com/doi/10.1029/1999PA900001 by Mbl Whoi Library, Wiley Online Library on [11/11/2022]. See the Terms and Conditions (https://onlinelibrary.wiley.com/terms-and-conditions) on Wiley Online Library for rules of use; OA articles are governed by the applicable Creative Commons License

References

Adkins, J F , and E A Boyle, Changing atmospheric $\Delta^{14}C$ and the record of deep water paleoventilation ages, *Paleoceanography, 12*, 337-344, 1997.

Bauch, D , P Schlosser and R G. Fairbanks, Freshwater balance and the sources of deep and bottom waters in the Arctic Ocean inferred from the distribution of $H_2{}^{18}O$, *Prog. Oceanogr*, 35, 53-80, 1995

Bemis, B E , H J Spero, J Bijma, and D W Lea, Reevaluation of the oxygen isotopic composition of planktonic foraminifera Experimental results and revised paleotemperature equations, *Paleoceanography, 13*, 150-160, 1998.

Boyle, E.A , Cadmium and $\delta^{13}C$ paleochemical ocean distributions during the stage 2 glacial maximum, *Annu Rev. Earth Planet. Sci., 20*, 245-287, 1992

Boyle, E A and L Keigwin, North Atlantic thermohaline circulation during the past 20,000 years linked to high-latitude surface temperature, *Nature, 330*, 35-40, 1987

Broecker, W S , Oxygen isotope constraints on surface ocean temperatures, *Quat. Res., 26*, 121-134, 1986.

Broecker, W S, et al , Accelerator mass spectrometry radiocarbon measurements on marine carbonate samples from deep-sea cores and sediment traps, *Radiocarbon, 30*, 261-295, 1988

Craig, H , and L I Gordon, Deuterium and oxygen 18 variations in the ocean and the marine atmosphere. Stable isotopes in oceanographic studies and paleotemperatures, in *Proceedings of the Third Spoleto Conference, Spoleto, Italy*, edited by E Tongiori, pp 9-130, Sischi and Figli, Pisa, Italy, 1965.

Curry, W B , Late Quaternary deep circulation in the western equatorial Atlantic in *The South Atlantic: Present and Past Circulation*, edited by G Wefer et al., Springer-Verlag, New York, 1997

Curry, W.B , N C Slowey, and G P. Lohmann, Oxygen and carbon isotopic fractionation of aragonitic and calcitic benthic foraminifera on Little Bahama Bank, Bahamas, EOS, *Trans. AGU, 74*, (43), Fall Meet Suppl., 368, 1993

Duplessy, J C , N J Shackleton, R G Fairbanks, L. Labeyrie, D Oppo and N Kallel, Deepwater source variations during the last climatic cycle and their impact on the global deepwater circulation, *Paleoceanography, 3*, 343-360, 1988

Emiliani, C , Depth habitats of some species of pelagic foraminifera as indicated by oxygen isotope ratios, *Am J. Sci., 252*, 149-158, 1954

Emiliani, C , Pleistocene temperatures, *J. Geol., 63*, 538-578, 1955

Fairbanks, R.G , M. Sverdlove, R Free, P H. Wiebe, and A W H Be, Vertical distribution and isotopic composition of living planktonic foraminifera from the Panama Basin, *Nature, 298*, 841-844, 1982

Fairbanks, R G., C D Charles and J D Wright, Origin of global meltwater pulses, in *Radiocarbon after Four Decades*, edited by R E. Taylor et al., pp 473-500, Springer-Verlag, New York, 1992.

Fofonoff, N P , Dynamics of ocean currents, in *The Sea: Ideas and Observations on Progress in the Study of the Seas*, vol 1, *Physical Oceanography*, edited by M.N Hill, pp 323-395, John Wiley, New York, 1962

Gardner, W D , M J. Richardson and D A. Cacchione, Sedimentological effects of strong southward flow in the Straits of Florida, *Mar. Geol., 86*, 155-180, 1989

Herguera, J C , E Jansen, and W.H Berger, Evidence for a bathyl front at 2000-m depth in the glacial Pacific, based on a depth transect on Ontong Java Plateau, *Paleoceanography, 7*, 273-288, 1992.

Hogg, N G , and W E Johns, Western boundary currents, *Rev. Geophys , 33*, 1311-1344, 1995

Johns, E , D R Watts and H T Rossby, A test of geostrophy in the Gulf Stream, *J. Geophys. Res., 94*, 3211-3222, 1989

Joussame, S and J Jouzel, Paleoclimatic tracers An investigation using an atmospheric general circulation model under ice age conditions, 2, Water isotopes, *J. Geophys. Res., 98*, 2807-2830, 1993.

Kim, S -T , and J. O'Neil, Equilibrium and nonequilibrium oxygen isotope effects in synthetic carbonates, *Geochim. Cosmochim. Acta, 61*, 3461-3475, 1997

Labeyrie, L D , J.-C. Duplessy, J Duprat, A Juillet-Leclerc, J Moyes, E Michel, N. Kallel and N J Shackleton, Changes in the vertical structure of the North Atlantic Ocean between glacial and modern times, *Quat. Sci. Rev., 11*, 401-413, 1992.

Larsen, J.C , Transport and heat flux of the Florida Current at 27°N derived from cross-stream voltages and profiling data. Theory and observations, *Philos. Trans. R. Soc. London, Ser. A, 338*, 169-236, 1992.

Leaman, K D , E Johns, and T Rossby, The Average Distribution of Volume Transport and Potential Vorticity With Temperature At 3 Sections Across the Gulf-Stream, *Journal of Physical Oceanography, 19* , 36-51, 1989

Levitus, S., and T.P Boyer, *World Ocean Atlas 1994*, Nat Oceanic and Atmos Admin , Silver Spring, Md , 1994.

Locker, S.D , and A C Hine, Late Quaternary sequence stratigraphy, South Florida margin, paper presented at the 27th Annual Offshore Technology Conference, Houston, Tex , 1-4 May, 1995

Lynch-Stieglitz, J., and R G Fairbanks, A conservative tracer for glacial ocean circulation from carbon isotope and paleo-nutrient measurements in benthic foraminifera, *Nature, 369*, 308-310, 1994

McIntyre, A , N G Kipp, A.W H Be, T.J Crowley, T Kellogg, J V. Gardner, W. Prell, W. and W F. Ruddiman, The glacial North Atlantic 18,000 years ago A CLIMAP reconstruction, in *Investigation of late Quaternary Paleoceanography and Paleoclimatology*, edited by R.M Cline, and J D. Hays, *Geol. Soc. Am. Mem., 145*, 43-76, 1976

Millero, F J , and A Poisson, International one-atmosphere equation of state of seawater, *Deep Sea Res., Part A., 28*, 625-629, 1981

O'Neil, J.R , R N Clayton, and T K. Mayeda, Oxygen isotope fractionation in divalent metal carbonates, *J. Chem. Phys., 5*, 5547-5558, 1969

Ortiz, J D , A C. Mix, S Hostetler and M Kashgarian, The California Current of the Last Glacial Maximum: Reconstruction at 42°N based on multiple proxies, *Paleoceanography, 12*, 191-206, 1997

Pillsbury, J.E., The Gulf Stream—A description of the methods employed in the investigation, and the results of the research, *Rep. U.S. Coast Geod. Surv., 10*, 459-620, 1891

Pond, S , and G.L Pickard, *Introductory Dynamical Oceanography*, 329 pp , Pergamon, Tarrytown, N Y , 1983.

Richardson, W.S , W J Schmitz Jr , and P P Niiler, The velocity structure of the Florida Current from the Straits of Florida to Cape Fear, *Deep Sea Res.*, Suppl. to *16*, 225-231, 1969

Rosenthal Y., E A Boyle and N Slowey, Temperature control on the incorporation of magnesium, strontium, fluorine, and cadmium into benthic foraminiferal shells from Little Bahama Bank: Prospects for thermocline paleoceanography, *Geochim. Cosmochim. Acta, 61*, 3633-3643, 1997.

Sarnthein, M , K. Winn, S J.A Jung, J C Duplessy, L. Labeyrie, H Erlenkeuser, and G Ganssen, Changes in East Atlantic Deep-Water Circulation Over the Last 30,000 Years - 8 Time Slice Reconstructions, *Paleoceanography, 9* (2), 209-267, 1994

Sato, O T., and T. Rossby, Seasonal and low frequency variations in dynamic height anomaly and transport of the Gulf Stream, *Deep Sea Res. Part I., 42*, 149-164, 1995.

Schmitz, W.J., and M S McCartney, On the North Atlantic circulation, *Rev. Geophys., 31*, 29-49, 1993.

Schmitz, W J., J R. Luyten and R.W Schmitt, On the Florida Current T/S envelope, *Bull. Mar. Sci., 53*, 1048-1065, 1993

Shackleton, N J , Attainment of isotopic equilibrium between ocean water and the benthonic foraminifera genus Uvigerina Isotopic changes in the ocean during the last glacial, *Cent. Nat. Rech., Sci Colloq. Int., 219*, 203-209, 1974

Shackleton, J J , J -C. Duplessy, M. Arnold, P Maurice, M A Hall, and J Cartlidge, Radiocarbon age of the last glacial Pacific, *Nature, 335*, 708-711, 1988

Slowey, N C , and W B Curry, Glacial-interglacial differences in circulation and carbon cycling within the upper western North Atlantic, *Paleoceanography, 10*, 715-732, 1995

UNESCO, Processing of oceanographic station data, Joint Program on Oceanogr Tables and Stand , 138 pp., Paris, 1991

Wust, G , Florida- und Antillenstrom Eine hydrodynamische Untersuchung, *Geogr. Natur. Reihe, 12*, 1-48, 1924

W B Curry, Woods Hole Oceanographic Institution, Woods Hole, MA 02543 (wcurry@whoi edu)

J Lynch-Stieglitz, Lamont-Doherty Earth Observatory, Palisades, NY 10964. (jean@ldeo columbia edu)

N Slowey, Department of Oceanography, Texas A&M University, College Station, TX 77843 (slowey@ocean tamu edu)

(Received September 21, 1998, revised December 30, 1998, accepted December 31, 1998)

19449186, 1999, 3, Downloaded from https://agupubs.onlinelibrary.wiley.com/doi/10.1029/1999PA900001 by Mbl Whoi Library, Wiley Online Library on [11/11/2022]. See the Terms and Conditions (https://onlinelibrary.wiley.com/terms-and-conditions) on Wiley Online Library for rules of use; OA articles are governed by the applicable Creative Commons License